Micro-Optic Applications in Food, Textile and Geo Sciences

Micro-Optic Applications in Food, Textile and Geo Sciences

By

Howard Swatland

Cambridge
Scholars
Publishing

Micro-Optic Applications in Food, Textile and Geo Sciences

By Howard Swatland

This book first published 2026

Cambridge Scholars Publishing

Lady Stephenson Library, Newcastle upon Tyne, NE6 2PA, UK

British Library Cataloguing in Publication Data
A catalogue record for this book is available from the British Library

ISBN: 978-1-0364-6244-4
ISBN (Ebook): 978-1-0364-6245-1

CONTENTS

MICRO OPTIC APPLICATIONS

All animals with eyes and all plants with a photosynthetic exposure are exploiting micro-optics. Things moved into the industrial world as the curiosity that followed the invention of the microscope matured into other inventions that we are now all dependent upon, such as display screens for televisions, computers and portable telephones. The technical literature for these industries is too vast to contemplate, even for works in the public domain. But micro-optics is also a way of investigating things, from food science to ecology, where fibre optics and microscopy have yielded a wide variety of results. This book is a compilation of my published research, bringing everything together in one place and exploring unsuspected optical similarities between unlikely applications such as measuring meat toughness and watching travertine precipitate on mosses in a waterfall. The chapters use text and figures as first submitted for publication in refereed journals and books before the restrictions of copyright laws.

Chapter 1 was a challenge. Clearly something would have to be included about microscope optics, but there are countless books about microscope optics. The solution was to adopt a new approach to the topic, using one the newest solar cells (perovskite) as the sample in a light microscope. Thus, as the light microscope was put through its paces, the responses of the sample could be measured electrically.

Chapter 2 considers fibre optics, not from their dominant use in telecommunications, but in the way they may be applied to answer many new questions in animal tissue structure and ecology.

Chapter 3 describes the importance of photometer responses. If a fibre optic probe is passing through animal tissues, or an optical fibre is being used to look at bubbles in flowing water, then the photometer must be a fast responder.

Chapter 4 uses a continuous inference filter as a monochromator.

Chapter 5 connects a photodiode array to the microscope.

Chapter 6 uses a UV diode for illumination.

Chapter 7 reviews how a promising UV probe to predict meat toughness did not work industrially. It was too sensitive to the anatomy of where it was applied.

Chapter 8 takes on the problem of relating the colour of wood to its microstructure.

Chapter 9 uses microscopy and fibre optics to measure red textiles.

Chapter 10 gets into starch, beyond just using optical fibres to measure emulsification in food products, but trying to explain how starch granules produce such fascinating patterns in polarized light.

Chapter 11 explains how light penetrates flowing water, with or without bubbles.

Chapter 12 uses polarized light interferometry to look at the formation of travertine – the white crust of calcium salts sometimes found in mosses around waterfalls.

Chapter 13 investigates coloured clays and arrives at an unexpected conclusion.

Chapter 14 looks at underwater shadowing by moss leaves. Terrestrial shadowing in ecology is difficult enough, all those flicker patterns from tree leaves, how should they be integrated to explain the light reaching the forest floor?

Chapter 15 uses micro-optics to look at the colours and fluorescence of natural latex.

Chapter 16 introduces electromechanical stages as a way to undertake basic research in histochemistry and then to connect to optical fibres for goniophotometry.

Chapter 17 takes goniophotometry to new level – moving the recording optical fibre towards the illuminating fibre.

Chapter 18 is a homage to Robert Hooke who first got us into using micro-optics to investigate the otherwise invisible World we live in.

CHAPTER 1

MICROSCOPY

It would take a very large college of science historians, physicists and mathematicians to identify the start point and key paradigm shifts of optics. But the start point of applications for micro optics is much easier. It starts in 1665 with Robert Hooke's book *Micrographia*. Great discoveries have been made by biologists and medical scientists without perhaps knowing the mathematical optics of their microscopes? This book is about applications and contains nothing about explaining micro-optics mathematically. But just as Robert Hooke had a good understanding of how lenses might be used to investigate something of interest, we need to understand empirically a little about the tools we are using.

Anyone with access to the internet may obtain an unreadable number of books and research papers about the physical optics of light microscopy. But these are all based on optical engineers and physicists looking down microscopes to explain what may be observed. Here we take a novel approach and ask what is it like to be a specimen examined in a light microscope? For living creatures the answer is simple – we will most likely get cooked by the heat produced by the illuminator. But here we will use a robust perovskite solar cell as our sample.

Testing the components of a computer assisted light microscope may reveal their operational characteristics to the advantage of the programmer [1]. This is particularly important for the timing of operations such as fluorometry where fading or quenching may occur while a spectrophotometer is advancing. Hence, photomultiplier response times may be monitored [2] or a photomultiplier may be replaced by a photodiode array spectrograph [3].

A solar cell generating electricity when illuminated makes many new tests possible. Instead of regarding the sample under the microscope as a passive target, it now becomes an active part of the whole system, and it is now possible to gather new information about the illumination of the sample. But first this requires a study of the solar cell as a micro sensor

rather than a source of macroscopic power. The key point is that the solar cell is designed to be fully illuminated, but when used as a sensor on a microscope stage it is partly illuminated with the dark area acting as a resistor. What is the most useful output – volts or amps? There is a massive amount of published information on microscope photometry [4] and perovskite solar cells [5], but with a few simple questions and experiments we may advance on a path into a new territory. Whether the path leads anywhere or whether it is merely curious cul-de-sac remains to be seen. A fantastic amount of money is now being spent on the development of solar energy, looking at energy production from planetary areas of solar cells, but is it possible that light microscopy of a microscopic area might reveal anything? It certainly helps with microscopy, as expounded below.

Microscope

The microscope was a Zeiss Universal with reflectance attachments. Early information gathered from the perovskite solar cell was used to help in developing the apparatus. Thus, apparatus and results are intermingled. An overall plan of the apparatus is given in Fig. 1,1, with technical details evolving as data collection advanced. Details of microscope parts and software are available [1].

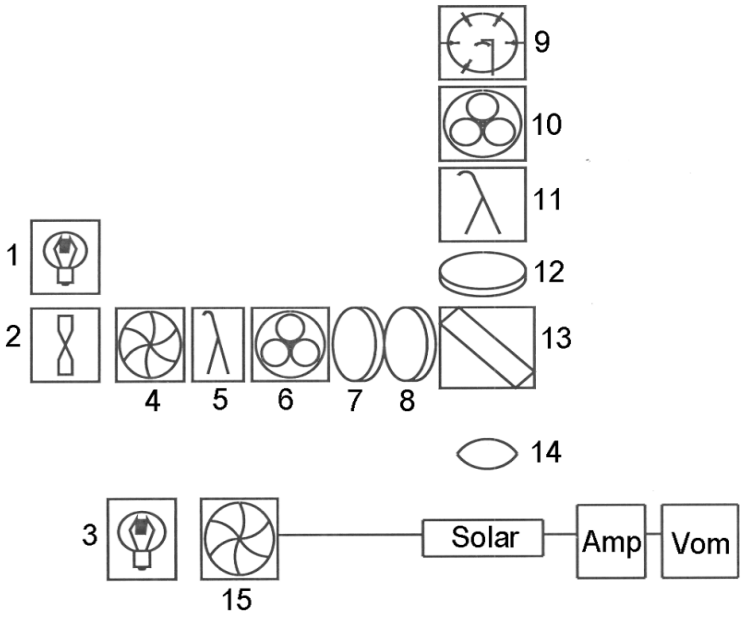

Fig. 1, 1. Apparatus. Interchangeable illuminators with tungsten bulbs, xenon arcs or UV LEDs (1 – 3), solenoid shutters (4 and 15), grating monochromators (5 and 11), stray-light filters for monochromators (6 and 10), polarizer (7), optional quarter-wave plate (8), photomultiplier (9), motorized analyzer (12), beam splitter (13), microscope objective lens (14) and perovskite solar cell (Solar) linked with an amplifier (Amp) and voltmeter with oscilloscope (Vom).

Beam splitter

Possibilities for the beam splitter as a reflector for vertical bright field illumination are shown in Fig.1, 2. One may use a flat partial reflector with anti- and semi-reflecting films (Fig. 1,2,1), a mirror before the partial reflector as invented by Smith [6] (Fig.1,2, 2), or a Berek double prism full reflector [7] (Fig.1,2, 3). Options 1 and 2 allow the full use of the resolving power of the objective and uniform illumination but there is a loss of light intensity from axial beam splitting. Option 3 allows only half the objective aperture and may vignette high-power objectives, but light intensity is brighter than options 1 and 2 because the beam has been spatially separated and not split axially. Are these predictions detectable by a perovskite solar cell?

The answer is most certainly yes. Comparing a partial mirror reflector (Fig.1, 2, 1) with a Berek prism full reflector (Fig.1, 2, 3) the voltage output from the solar cell minus a correction for ambient light was, respectively, 3.05 ± 0.005 mv versus 4.19 ± 0.017 mv ($P < 0.001$, $n = 100$). This was with white light from a 100 w tungsten source and a LD-EPIPLAN objective (× 4, NA 0.1) and with volts amplified. Volts gave a better statistical separation than amps ($t = 6.43$ *versus* $t = 4.92$, respectively). A similar response was found with higher power objectives (up to × 40).

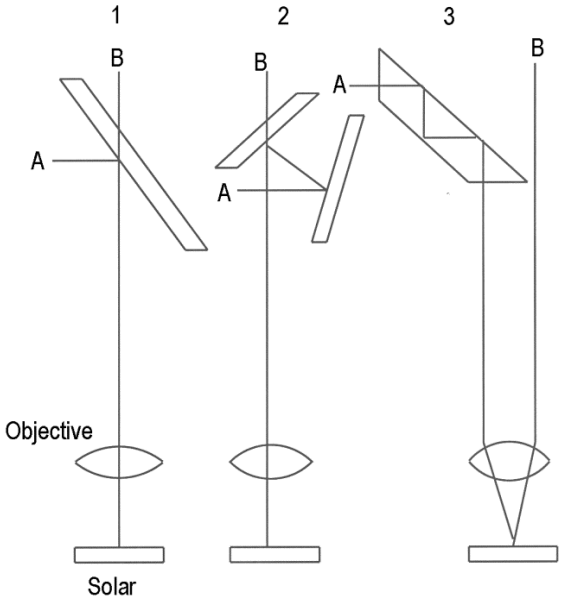

Fig. 1, 2. Possibilities for a beam splitter above the solar cell to give vertical bright field illumination, a simplified diagram from Horst Piller [5]. Collimated beam from an illuminator (A) and reflected light to the photomultiplier (B). Either planar glass with anti- and semi-reflecting films (1), a reflector mirror before the planar glass (2), or a Berek prism reflector [10] (3).

Surface Reflectance

The surface of the perovskite solar cell (Ixolar SM141K06L R3.0, Anysolar, Republic of Korea) was randomly covered by numerous brightly reflective structures ranging up to approximately 30 μm across (Fig. 1, 3).

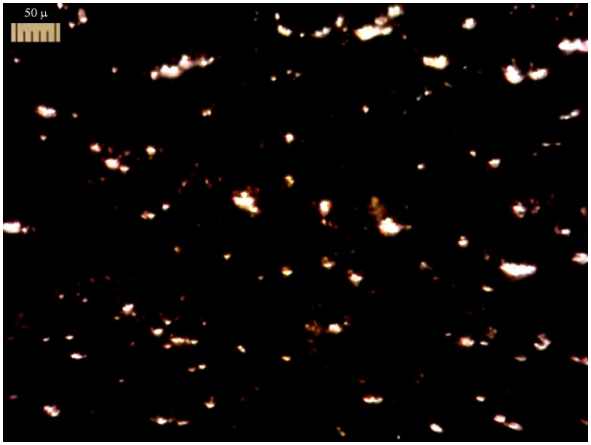

Fig. 1, 3. The surface of a perovskite solar cell illuminated laterally at 45°.

These bright spots were investigated using vertical illumination through a beam splitter and a vertical photometry pathway through the apparatus passing through a grating monochromator with stray light filters to a photomultiplier (Fig. 1, 1). The apparatus was standardized (reflectance = 1 from 400 to 700 nm in 10 nm steps) on 5 layers of white Teflon tape that had a diffuse or Lambertian appearance. The bright spots had about 0.3 of the reflectance of Teflon and were significantly ($P < 0.001$) brighter than the dark back ground (Fig. 1, 4). The solar cell was reading 3.97 mv. The reflectance spectrum of the bright spots was almost flat, thus suggesting this was specular or Fresnel reflectance. The dark background showing light entering the solar cell peaked at 400 nm but the difference between 400 and 700 nm was not statistically significant ($t = 1.61$).

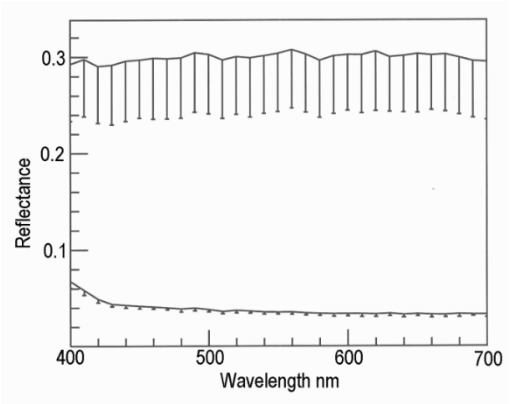

Fig. 1, 4. Reflectance of bright spots in Fig. 3 (top line) *versus* dark background (bottom line). Error bars are standard deviations (n =10) measured with a ×40 Epiplan objective.

To confirm that the bright spots were from Fresnel reflectance, they were illuminated with plane polarized light and the analyzer was rotated, as shown in Fig. 1,5. Thus, this particular perovskite solar cell was losing a little energy by reflection. Was it from imperfections in the float glass top layer, who knows? But as a sensor in a polarizing microscope, what about the light entering the solar cell?

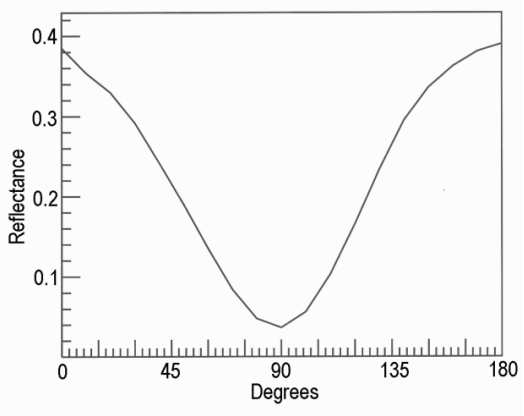

Fig. 1, 5. Reflectance of a bright spot from Fig. 3 illuminated with plane polarized light and modulated by a rotary analyzer in the photometry pathway (Fig. 1, 1, 7), using a ×40 Epiplan objective.

For Fig. 1, 5, the microscope was used normally with illumination through the beam splitter and reflected light being passed through the motorized analyzer (Fig. 1, 1, 12). But to use the analyzer to rotate the plane of polarization of light on the perovskite solar cell, the optical axis of the microscope was inverted by substituting an illuminator in the place of the eyepiece. Thus, light from the illuminator passed through the analyzer to illuminate the perovskite solar cell whose voltage output was found from the amplifier (Fig. 1, 1, Amp and Vom). To check that the results did not originate from strained glass components in this unusual optical pathway, rotation of a polarizer placed directly on the perovskite solar cell gave comparable results. As shown in Fig. 1, 6, the perovskite solar cell was sensitive to the plane of polarized light, as well as to elliptically polarized light created by retarders in the light path across a wide range of illumination intensities [8].

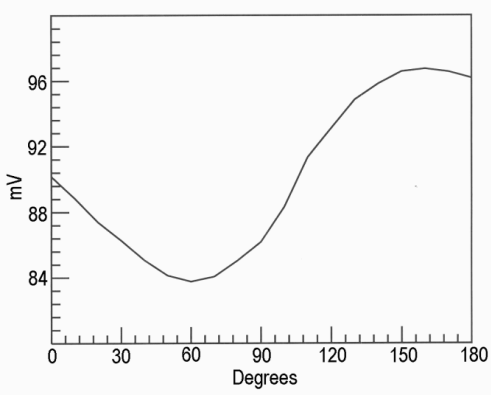

Fig.1, 6. Modulation of the voltage produced by the perovskite solar cell with an analyzer rotating plane polarized light.

A side analysis of a perovskite solar cell

This research project was started with a simple question – can a perovskite solar cell be used to understand more about how a microscope functions in directing light to a sample? The answer was yes. Quartz optics for UV in a prism beam splitter (Fig.1, 2, 3) reduced the visible light on the sample, and numerical apertures in objective lenses gave predictable responses, and dichroic beam splitters from old fluorescence microscopes were not much different than simple reflectors (because of the flat response of perovskite across the visible spectrum). No point in giving the statistics

because these components are now ancient history and few people use them. But curiosity beckons.

Microscope photometry is best done at a constant cool temperature in very dim ambient light to minimize thermionic noise and stray light reaching a sensitive photomultiplier. But with an old computer without illuminated keys, a small illuminator on the keyboard is required away from the microscope, and it is also needed to write down operating data and to prepare samples. For any measurement at different wavelengths or planes of polarization, it is highly desirable to use a shutter to measure the dark field current and to subtract it from photometric data (using shutters as in Fig. 1, 1; 4, 10 and 15). Looking at dark field currents critically, it did not take long to find that dim lateral illumination of the perovskite chip was producing a noticeable effect on the dark field voltage from the photomultiplier (shutters closed). So following the exploratory logic of inverting the vertical axis of the microscope (illuminating the sample through the eyepiece pathway as in Fig. 1, 6), curiosity beckoned – how might a perovskite solar cell function as a sensor if rotated 90° so that light entered sideways into the multiple layers of the chip [5] instead of onto the top surface?

Manufacturer's data show that perovskite solar cells have an admirable flat response across the visible spectrum, but does this hold true for light entering from the edge of the solar cell? With light from a xenon arc passed through a grating monochromator with stray light filter to remove high-order harmonics, the flat response held true, with only a very slight maximum response around 500 nm (Fig. 1, 7).

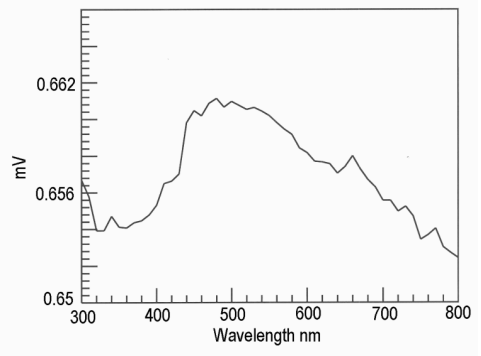

Fig. 1, 7. Expanded graphics of essentially a straight line relationship for voltage output from the perovskite solar cell across the spectrum when illuminated from the edge of the chip, not from the top surface of the chip as in normal use.

The side analysis of the perovskite solar cell at different wavelengths (Fig. 1, 7) revealed that the perovskite layer of the cell [8] was strongly fluorescent in UV light. Fluorescence emission was measured using a dichroic beam splitter previously found to give 4.28 mV on the cell with visible light. The illuminator was a 100 W mercury arc with a UG5 barrier filter to remove visible light. UV illumination at 365 nm on a small point of the side of the cell gave 3.08 mv, almost as much as full illumination on the top surface of the cell with visible light (4.28 mV). The system was checked by measuring the fluorescence of uranyl glass. The peak fluorescence of perovskite was at 510 nm, the flat top to the emission spectrum was caused by only stepping the grating monochromator at a band-width of 10 nm (Fig. 8). There is a compromise here, lesser band-widths reduce the amount of light to be measured. The objective lens was an Epiplan Neofluar, × 16, NA 0.5 at 1 mm.

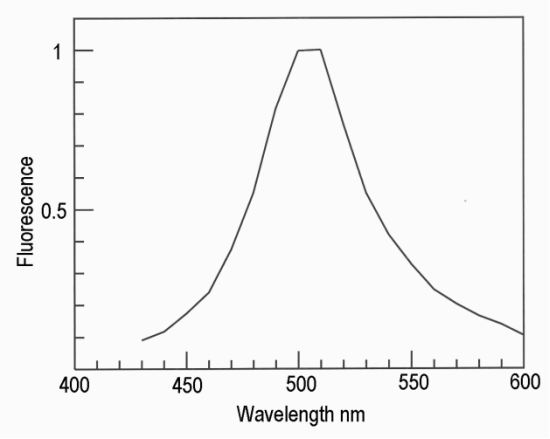

Fig. 1, 8. Normalized fluorescence emission of the perovskite layer on the side of a solar cell.

Discussion

In the spirit of Robert Hooke, who looked at anything curious under his microscope, we now have available some amazing products of technology to investigate. Vast areas of our planet are now covered by silicon cells generating electricity. Perovskite solar cells might be next, if their problems can be overcome. Taking a perovskite cell the size of a large postage stamp and looking at it under a light microscope was an attractive

idea. When I started, I never would have guessed it would have encouraged me to invert the optics of a light microscope – illuminating a specimen through the eyepiece optics, or rotating a solar cell 90° to investigate light entering laterally. But the data are here for you to see. I certainly understand my microscope better than when I started.

Conclusions

A perovskite solar cell may be used on the stage of a light microscope to assess the light intensities reaching the sample with different optical systems. Perovskite solar cells have an almost flat response across the visible spectrum, but are sensitive to polarized light. When tested from the side of a chip, the perovskite layer generates a voltage and is strongly fluorescent.

References

1. Swatland, H.J. (1998) *Computer Operation for Microscope Photometry*. CRC Press, Boca Raton, Florida, USA.
2. Swatland, H.J. (1993) Photomultiplier response in a computer-assisted microscope photometer measured with a multiprogrammer. *Journal of Computer-Assisted Microscopy*. **5**: 231-235.
3. Swatland, H.J. (1995) Microscope spectrofluorometry of bovine connective tissue using a photodiode array. *Journal of Computer-Assisted Microscopy*. **7**:165-170.
4. Piller, H. (1977) *Microscope Photometry.* Springer-Verlag, Berlin.
5. Mahapatra, A., Prochowicz, D., Tavakoli, M.M., Trivedi, S., Kumar, P. and Yadav, P. (2019) A review of aspects of additive engineering in perovskite solar cells. *Journal of Materials Chemistry A.* DOI: 10.1039/c9ta07657c
6. Smith, F.H. (1964) A new incident illuminator for polarizing microscopes. *Mineral Magazine* **33**, 725-729.
7. Berek, M. (1936). Ein Prisma für 90° - Ablenkung, be idem die Störungen im Polarisations zustand eines wenig geöffneten räumlichen Stralenbündelskorrigiert sind. *Zeischrift Instrumentkunde.* **56**, 1-6.
8. Wang, X., Wang, Y., Gao, W., Song, L., Ran, C. and Huang,W. (2021). Polarization-sensitive halide perovskites for polarized luminescence and detection: recent advances and perspective. *Advanced Materials.* 33 (12). https://doi.org/10.1002/adma.202003615

CHAPTER 2

FIBRE OPTICS

Summary

In telecommunications, there are tools and tricks to link optical fibres together in a way that eliminates distortion of a square wave of monochromatic light. But in many fibre optic applications, the fibres must be cut and polished elliptically to exit from the side of a needle probe, and fibres may be carrying wavelengths across the spectrum as a continuous analogue signal. The final departure from normal fibre optic protocols is that beyond the terminal window of the fibre may be a complex optical system such as a translucent tissue or moving water. Using optical fibres as sensors, we also need to consider how light returned from the sample is to re-enter a single fibre or be collected by an adjacent fibre.

A computer-assisted light microscope with a vertical illuminator for reflected light was used to investigate internal Fresnel reflectance at the distal (far) window of an optical fibre. Reflectance from the proximal (near) window was minimized by crossed polars in the illuminating and image forming pathways. Although light scattered in the optical fibre contributed to light reflected internally from the distal window, the latter could be identified by changing the cutting angle and refractive index at the distal window. Internal reflectance was correlated negatively with the refractive index of sucrose solutions at the distal window (at 500 nm, $r = 0.92$, $P < 0.005$). Minimum internal reflectance occurred when the distal window was cut at 75^{o} to the long axis of the fibre, and the maximum was at 30 or 45^{o}.

Introduction

Optical fibres have many applications in medicine and biology because they enable a variety of optical measurements to be made directly on biological tissues [1]. However, when optical fibres are interfaced directly with tissues, it is difficult to predict the optical properties of the optical window and of the tissues beyond. The refractive index of the fluid phase of a biological sample

may affect the Fresnel reflectance losses at the optical window, as occurs in the coupling of optical fibres used for communication [2]. When passing from medium x to y, with refractive indices n_x and n_y,

$$\text{Fresnel loss (dB)} = 10 \log ((2 + (n_x / n_y) + (n_y / n_x)) / 4)$$

But both refractive index and the transmittance of optical fibres are related to wavelength, so it is difficult to predict how white light will be transmitted into a medium that may vary in refractive index.

Optical fibres used for communication generally are cut perpendicularly to the long axis of the fibre, but this may be unsuitable for certain biological applications. For example, if a fibre optic probe is to be pushed repeatedly into a tissue or semisolid product to make a routine measurement, the probe requires a cutting edge at its tip and the best location for the optical window is on the side of the shaft. Given that a narrow shaft has many advantages over a thick one, and that optical fibres have a limited radius of curvature, it may be necessary to terminate the fibres at acute angle at the optical window, rather than perpendicularly. What effect does this have on the optical properties of the window?

Relatively few wavelengths are used for digital communication through optical fibres and reflectometers for testing fibre-optic connections are poorly suited for the analysis of analog information in multimode fibres. This chapter describes how a computer-assisted light microscope may be used for this purpose.

Apparatus

A block diagram is given in Fig. 2, 1.

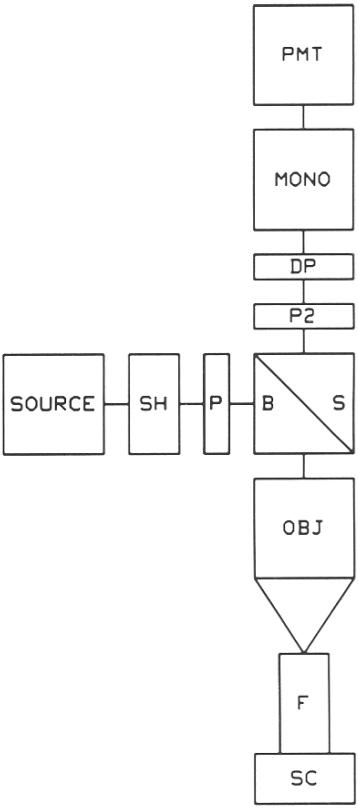

Fig. 2, 1. Block diagram of apparatus. Source of light, SOURCE; solenoid-operated shutter, SH; illumination-side polar, P; beam splitter, BS; microscope objective lens, OBJ; optical fibre, F; sample chamber, SC; measuring-side polar, P2; depolarizer, DP; monochromator, MONO; and photomultiplier, PMT.

The light source (SOURCE in Fig. 2, 1) was a short-arc xenon with stabilized power supply using a solenoid-operated shutter (SH in Fig. 1) to find the dark-field current of the photomultiplier. The collimated light from the source passed through a polar (P in Fig. 2, 1) and into a strain-free beam splitter (BS in Fig. 2, 1). A Neofluar objective (OBJ in Fig. 2, 1) was focused on the proximal window of a 1-m length of 1-mm diameter plastic optical fibre (Hewlett-Packard HFBR; F in Fig. 2, 1). The distal end was inserted into the axis of a pyrex glass sample chamber (internal diameter 25 mm; SC in Fig. 2,

1). The fluid in the sample chamber (depth 4 cm) was flushed with a continuously variable concentration of analytical grade sucrose solution that was calibrated in series by passing through the continuous flow cell of an Abbe refractometer.

Reflectance from the proximal window of the optical fibre was minimized with a second polar (P2 in Fig. 2, 1) on the measuring side of the beam splitter. The second polar was rotated to obtain the minimum reflectance from the proximal window. Light internally reflected from the distal window, together with light reflected by scattering within the optical fibre, was passed through a depolarizer (DP in Fig. 2, 1), through a grating monochromator with an automatic filter changer for stray light, and onto a side-window photomultiplier (PMT in Fig. 2, 1). It is assumed that some of the light returning back up the optical fibre was lost by internal reflection at the proximal window.

The monochromator was incremented from 400 to 700 nm in steps of 10 nm with a band pass of 10 nm. With the distal window of the optical fibre in air (facing black paper in a room with a low level of ambient light), the dynamic range of the photomultiplier was set at 470 nm. Then the monochromator was scanned from 400 to 700 nm to standardize the system so that light reflected from the fibre (internal reflectance at the distal window + scattering in the fibre + residual reflectance at the proximal window) = 1 at each wavelength. The refractive index experiment was replicated four times. The fourth replicate reported here was obtained after a minor source of error had been eliminated (formation of minute bubbles on the fibre optic window immersed in the sucrose solution). Sucrose solutions are optically active, but the plane polarized light entering the multimode fibre was assumed to be depolarized by the time it reached the distal window.

For the experiment on cutting angle, optical fibres were cut under a dissecting microscope using scalpel and razor blades to obtain a smooth surface, but not completely free from irregularities. Compared to fibres sanded with 600 grit-paper [3], this gave a 1.13 dB increase in internal Fresnel reflectance. The cutting experiment resulted in small losses (<5 mm) in the length of the optical fibre, but the loss in length of fibre per se was imperceptible compared to the major effect of the angle of cutting.

Results

When the distal windows of optical fibres cut at 90^{o} were placed into distilled water, there was a decrease in reflected light (from A to F in Fig. 2,1). The

effect was stronger from 500 to 700 nm than at 400 nm. With a range from air (n = 1) to 63.5 % sucrose (n = 1.45), the decrease in reflectance was significant at all wavelengths (Fig. 2, 3, Table 2, 1). With a range from water (n = 1.333) to 63.5% sucrose, correlations of refractive index with light intensity were weaker, but still significant (Table 2, 1).

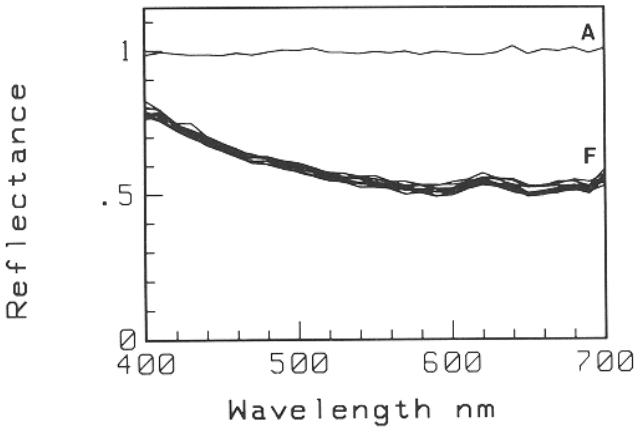

Fig. 2, 2. Reflectance from the distal window (90°) of an optical fibre in air (A) and in fluids (F) ranging from water (n = 1.333) to approximately 63.5% sucrose (n = 1.450)

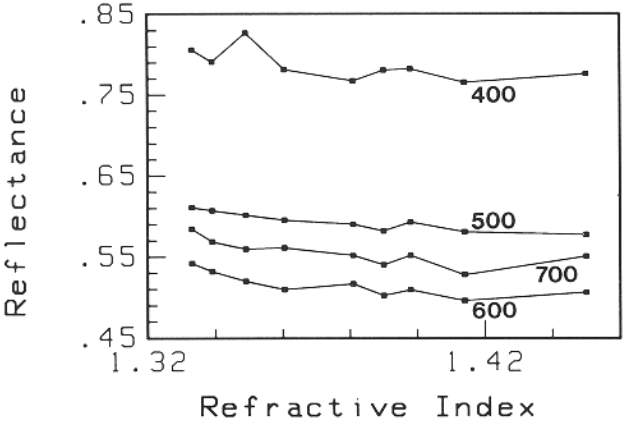

Fig. 2, 3. Reflectance from the distal window (90°) at 400, 500, 600 and 700 nm relative to fluid refractive index.

Table 2.1. Simple correlations of reflectance with refractive index.

λ nm	Range			
	From air to sucrose		From water to sucrose	
	Slope	r	Slope	r
400 0.64[a]	-0.51	-0.97[d]	-0.33	-
500 0.92[d]	-1.01	-0.98[d]	-0.29	-
600 0.78[c]	-1.17	-0.97[d]	-0.30	-
700 0.73[b]	-1.11	-0.97[d]	-0.31	-
	[a]$P < 0.05$, [b]$P < 0.025$, [c]$P < 0.01$, [d]$P < 0.005$			

The angle at which the distal window of the optical fibre was cut (relative to the long axis of the fibre) had a strong effect on internal reflectance from about 420 nm to 700 nm (for measurements made in air). However, as shown in Fig. 2, 4, the effect was negligible at 400 nm. For data at 600 nm, the results of three replicates of the experiment are shown in Fig. 5. Reflectance dropped when 15° was sliced off the perpendicular window. But, with continued removal of 15° segments, reflectance increased to reach a maximum at 45 or 30° of residual angle. Differences between the replicates were attributed to the difficulty of shaping the angles exactly by hand.

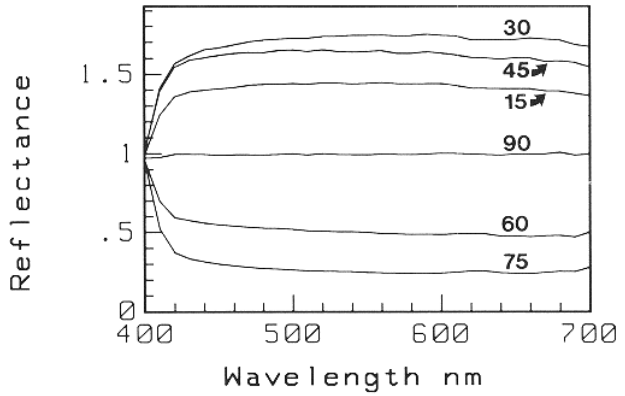

Fig. 2, 4. Effect of window angle (15 to 90° relative to the long axis of the fibre) on reflectance.

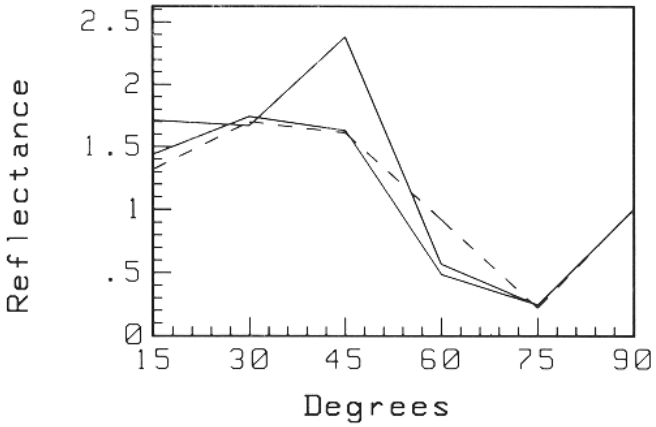

Fig. 2, 5. Effect of window angle on reflectance at 600 nm (three replicates of experiment shown in Fig. 2, 4).

Discussion

There are many problems yet to be solved for a proper understanding of the interface between optical fibres and tissues, but the results reported here are already useful in relation to probes used for predicting the chemical composition of meat. The type of fibre tested here is the same as that used in a UV fluorescence probe for connective tissue in beef [5], where a dichroic mirror is used to separate outgoing UV excitation into the fibre from the incoming light from the fluorescence of connective tissues appearing in the distal window of the fibre. The probe has a depth sensor so that the fluorescence signal can be analyzed as a transect through the tissues. The bidirectional use of a single optical fibre with a relatively large window solves the problem of light scattering in the sample. If separate outgoing and ingoing fibres are used they can only be linked by light passing through the tissue, which may be desirable for some applications, but not for fluorescence measurements which are best made directly at the window surface. With this bidirectional arrangement, the optical properties of the window may produce very large effects, which is what prompted this study.

Measurements of the refractive index of meat fluid have been made over a wide range of conditions [4], and the maximum range expected under normal conditions would be from about 1.3530 to 1.3650. From Fig. 2, 3, it may be seen that this will have only an imperceptible effect on optical properties at

the optical window. Thus, pH-related effects that have been detected are unlikely to originate from the relationship of pH with the refractive index of meat fluid, and the search must continue for its explanation.

Similarly, although Fig. 2, 5 shows that even relatively small changes in the cutting angle of the optical fibre may influence the optical properties of the window, the effect was negligible at 400 nm. This finding was re-checked down to 350 nm, and shown to hold true for the 365 nm mercury peak used as a source of fluorescence excitation in the UV probe. However, although cutting angle may have little effect on the emittance of UV light at 365 nm from the fibre, the data in Fig. 2, 5 show that the angle may affect the collection of fluorescence emissions (which are at wavelengths > 420 nm for connective tissue in skeletal muscle).

References

1. Kapany, N.S. (1967). *Fibre Optics. Principles and Applications*. Academic Press, New York.
2. Hewlett-Packard (1982). Digital data transmission with the HP fibre optic system. Application Note 1000, Hewlett-Packard, Palo Alto, CA.
3. Hewlett-Packard (1990). *Optoelectronics Designer's Catalog 1991-1992*. Hewlett-Packard, Palo Alto, Ca. p. 5-33.
4. Irie, M. and Swatland, H.J. (1992). Relationships between Japanese pork color standards and optical properties of pork before and after frozen storage. *Food Research International*. 25: 21-30.
5. Swatland, H.J. (1991). Analysis of signals from a UV fluorescence probe for connective tissue in beef carcasses. *Computers and Electronics in Agriculture*. 6: 225-234.

CHAPTER 3

PHOTOMETER RESPONSE

Summary

A multiprogrammer with an analog to digital converter triggered by a pulse train generator was used to follow the responses of a photomultiplier in a microscope photometer. Data were collected in parallel during the normal programmed operations of the system and were used to find the times required for equilibration of the photomultiplier. With short exposures through a camera shutter, the area under the signal peak from the photomultiplier and the width of the peak at half maximum amplitude were correlated with shutter speed, r = 1. Area and width were unchanged by operating conditions (high voltage, high gain *versus* low voltage, low gain), when corrected for differences in dark current, and did not change with wavelength when photomultiplier voltage and gain were constant. An iris shutter, with segments moving centrifugally from the optical axis, produced a signal with a faster rise than when using a solid, swing-out shutter that opened the aperture from the edge. The area of the photomultiplier response to a pulse of light through an iris shutter was used as a minimum exposure method to measure the fluorescence emission spectrum of a bovine collagen fibre. This reduced fluorescence quenching by reducing the total exposure time to 0.1 s for each wavelength measurement.

Introduction

In telecommunications fibre optics, the response of the diode to convert a square wave pulse of light in an optical fibre to an electrical square wave is precisely controlled when the diodes are manufactured. But when optical fibres are used for a variety of new applications, we need to know the characteristics of the photometer used. In most of my research, I have used photomultipliers. They may be vintage technology now, but they are easy to control with analogue electronics.

Computer-assistance is almost essential for the routine use of a microscope photometer so that, as foreseen by Piller [1], a typical system now has a controller and an interface, as well as a microscope equipped with monochromators, photometers and solenoid shutters. The general operation of each component in a microscope photometer is well described [1], but it may be useful to take a critical look at a component performing its normal function.

A microscope photometer may be programmed to make many different types of measurements, but it is difficult to control several operations simultaneously with only a single controller. Thus, it is difficult to make an uninterrupted continuous series of measurements from a photomultiplier at the same time that other devices such as shutters and monochromators are being operated. A multiprogrammer, with the capability for parallel processing of interface cards, may be used to overcome this problem so that programmed methodological studies may be undertaken while the photomultiplier is working at its assigned task. This allows the operator to examine the operation of the system itself, answering questions such as how long it takes for a photomultiplier to equilibrate after a shutter has been opened.

Apparatus

An overview of the system is shown in Fig. 3, 1. The main controller was linked via a bus to microscope interface to provide all the normal functions of a computer-assisted light microscope, including the operation of a photomultiplier (PMT in Fig. 3, 1). However, the PMT output also was connected directly to an A:D card in a multiprogrammer to provide a high-speed dual measuring system. The A:D card was triggered from a programmable pulse train generator (period accuracy ± 0.01%) which was used as the clock for time-based measurements. Data were stored on a 4 K memory card using FIFO pointers to upload to the controller at appropriate times. Multiprogrammer cards were programmed by the armed-card interrupt method.

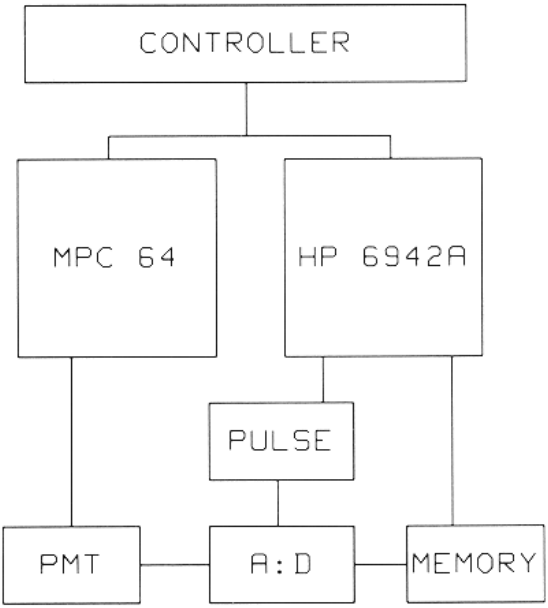

Fig. 3, 1. Block diagram of the system, showing the normal interface (MPC 64) between controller and photometer (PMT), and the parallel circuit created by the multiprogrammer containing a memory board buffering the output of an A:D converter triggered by a pulse-train generator.

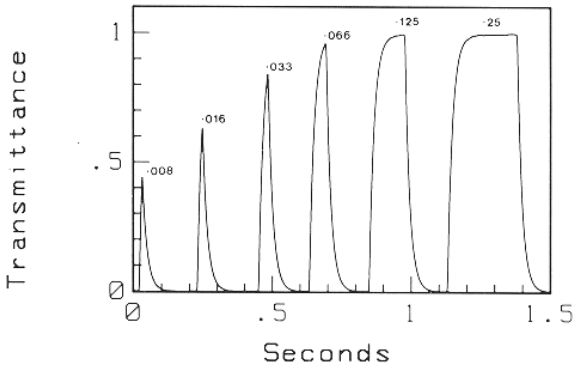

Fig. 3, 2. Photometer response to illumination modulated by a mechanical camera shutter (exposure times in seconds).

Photometer response to opening a shutter

A mechanical camera shutter (5-segment iris) mounted in the illumination pathway was used to test the system. Fig. 3, 2 shows the response of the photomultiplier to white light with a series of exposures of increasing duration (transmittance = 1 with continuous light). Using the high-speed A:D card in the multiprogrammer it was possible to follow the photomultiplier output and to find that a delay of about 0.1 s was required before taking a measurement through the normal circuit (Fig. 3, 3).

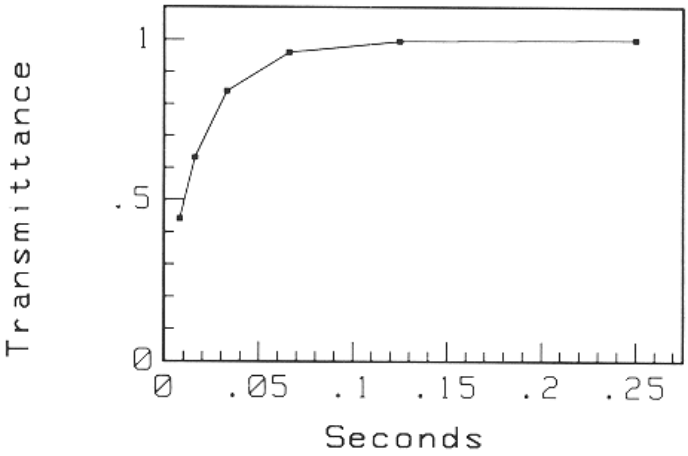

Fig. 3, 3. Effect of exposure time on maximum photometer response.

Fig. 3, 4 shows the effect of shutter speed on the area under the peak and the peak width at half its height. Area and peak width both were correlated with shutter speed, r = 1. Thus, for situations where photobleaching or deleterious sample responses may occur (as with living tissues), either area or peak width may be used to make rapid measurements without waiting for the photomultiplier to equilibrate. However, it cannot be assumed automatically that relationships such as those shown in Fig. 3, 4 will occur at all operating conditions. Do they change with wavelength, high-voltage or gain?